Curr Radiol Rep (2015) 3:45
DOI 10.1007/s40134-015-0128-6

Heating and Safety Concerns of the Radio-Frequency Field in MRI

Manuel Murbach[1] · Earl Zastrow[1,2] · Esra Neufeld[1] · Eugenia Cabot[1] · Wolfgang Kainz[3] · Niels Kuster[1,2]

Published online: 28 October 2015

Abstract Magnetic resonance imaging (MRI) is a widely used and powerful imaging technique for non-invasive clinical diagnosis. The absorbed radiofrequency (RF) energy must be carefully managed, as MRI presents one of the highest RF exposures to humans. Temperature increases in the patient caused by high-level RF exposure is a major safety concern in MRI, potentially causing local thermal tissue damage or systemic overheating. This review article summarizes recent findings in MR safety research, including the clear distinction between exposures of patients with and without implants; evaluates the advantages and limitations of numerical simulations for RF safety assessment in MRI; and discusses the need for additional research at high RF exposure levels and in novel MRI systems.

Keywords MRI safety · RF exposure · SAR · In silico assessment · Exposure assessment · Thermal dose

This article is part of the Topical Collection on *MRI Safety*.

✉ Niels Kuster
kuster@itis.ethz.ch

Manuel Murbach
murbach@itis.ethz.ch

Earl Zastrow
zastrow@itis.ethz.ch

Esra Neufeld
neufeld@itis.ethz.ch

Eugenia Cabot
cabot@itis.ethz.ch

Wolfgang Kainz
wolfgang.kainz@fda.hhs.gov

[1] IT'IS Foundation, Zeughausstrasse 43, 8004 Zurich, Switzerland

[2] Swiss Federal Institute of Technology (ETH), Rämistrasse 101, 8092 Zurich, Switzerland

[3] US Food and Drug Administration (FDA), Center for Devices and Radiological Health (CDRH), Silver Spring, MD 20993, USA

Introduction

Magnetic resonance imaging (MRI) has become a widely used diagnostic imaging tool in clinical practice. Radiofrequency (RF) exposure is considerably higher in a clinical MRI environment than in any non-clinical environment, requiring special considerations for RF safety. RF exposures from MRI are higher than recommended limits for occupational exposures and are orders of magnitude higher than those from fixed installations and mobile devices [1]. The product standard IEC 60601-2-33 ("particular requirements for the basic safety and essential performance of magnetic resonance diagnostic devices") [2] limits the RF exposure of MRI equipment. Although this standard has several gaps that are discussed below, MRI has a remarkable history of safe use (HoSU) with close to one billion scans performed since the first commercial MRI installation in the 80-ties, and overall reported severe incidents in the ppm region [3]. However, the overall duration of the vast majority of scans are much shorter than envisaged by IEC 60601-2-33, frequent scan interruptions are common, and manufacturers have implemented additional safety margins. Exposure to RF levels >85 % of the IEC limits (i.e., between 3.5 and 4 W/kg wbSAR) is reached on average for only 5 min during a scan [4], whereas the standard did allow 60 min at 4 W/kg until 2014. The current standard leaves any duration-related limit to the manufacturers' risk management. Therefore,

there is very limited HoSU for the full exploitation of the RF exposure limits in the IEC standard. Furthermore, emerging MRI technologies, such as parallel RF transmission (pTx, i.e., multi-channel transmit coils, [5•, 6]) and dynamic RF shimming [7], generate field distributions significantly different than traditional resonant body coils and, therefore, cannot rely on a HoSU.

The recently published Amendment 2 of IEC 60601-2-33 [2] extends the maximum upper limit of the first level controlled operating mode (OM) from 4 to 8 T. This review article focuses on traditional and predominantly used MRI scanners operating at 1.5 and 3 T. Ultra-high field MRI at 7 T and above pose additional safety concerns mainly due to the shorter RF wavelengths, as summarized in [8].

The RF pulse applied during MR imaging induces eddy currents in the human body and alters proton magnetization. The absorption of RF typically leads to exposure hotspots in areas with a high radial distance to the patient center, mainly in the arms/wrists, shoulder/neck, torso-lateral, groin, and in muscle constrictions, such as near the lateral pelvic bone. Additionally, anatomical RF loops resulting from contact between the hip and hand, for example, can significantly enhance the current density. Hotspots may also occur in close proximity to RF coil capacitors due to the capacitive coupling of the E-field or around the metal components of implants. The latter will be discussed separately, as the interaction mechanism is considerably different: an isolated metallic lead may "collect" RF energy along its trajectory and deposit it at its tip.

As the induced internal electromagnetic fields cannot be assessed experimentally in humans, validated in silico methods, i.e., simulations are used to determine the induced RF field distributions in vivo. Finite-difference time-domain (FDTD) and other finite-difference or finite-integration solvers have become the standard for electromagnetic and thermal simulations [e.g., Sim4Life (ZMT, Switzerland), SEMCAD X (SPEAG, Switzerland), and CST Microwave Studio (CST, Germany)], especially in high-resolution anatomical models such as the virtual population [9, 10]. Numerical estimations of RF energy deposition can be derived by adequately modeling the incident field of the MRI RF coil and by assigning tissue dielectric and thermal parameters based on literature values, e.g., from [11].

Global and local energy depositions in the tissues are typically defined in terms of the specific absorption rate (SAR), averaged over the whole-body (wbSAR), parts of the body (pbSAR), the head (hdSAR), or over any 10 g of tissue (psSAR10g). However, the induced temperature increase is only weakly related to SAR, as it is strongly influenced by the tissue-dependent blood perfusion rate. Furthermore, thermoregulation must be considered, as it becomes the most influential parameter with the high exposure levels in MRI [12]. For thermal stress or tissue damage, the relation to SAR is even weaker, as adverse thermal effects result from a combination of the induced temperature increase and exposure-duration, i.e., the thermal dose.

Current Safety Regime in MRI

The international standard IEC 60601-2-33 [2] defines temperature limits as basic restrictions, namely 40 °C in first level controlled operating mode (OM) and 39 °C in normal OM. This limitation applies to both core and local tissue temperatures; however, the rise of the core temperature cannot exceed 1 °C in first level controlled OM and 0.5 °C in normal OM. The standard also specifies derived SAR limits of 4 W/kg wbSAR, 3.2 W/kg hdSAR, and 4–10 W/kg pbSAR for first level controlled OM. While the whole-body exposure can be monitored via the overall power budget of the scanner, the local exposure cannot be assessed directly. Numerical simulations have shown that the derived SAR limits are not consistent with the basic temperature restrictions [13•, 14]. Some manufacturers voluntarily limit the psSAR10g via proprietary model predictions to avoid excessive local hotspots. Such estimations are typically derived from electromagnetic and thermal simulations using anatomical human models like the virtual population [9, 10].

RF Exposures

RF-induced exposures have been classified into two categories, "low-level RF exposure" and "high-level RF exposure" originating from: (a) long-term (chronic) low-level exposures, such as mobile phones or occupational exposures and (b) acute high-level exposures for typically shorter durations, such as MRI scans or medical hyperthermia treatments. Although chronic low-level RF exposures could be relevant for MR workers, they are probably not relevant to patients undergoing MRI exams. For completeness, we included them within the scope of this review article.

Low-Level RF Exposures

Low-level RF exposures originate from environmental sources, occupational sources, and personal devices. Environmental sources include broadcast antennas and base stations. Personal devices operating in close vicinity of the human body, such as mobile phones or access points, are the dominant sources of exposure. Persons exposed to

occupational sources include MR workers, military and security personnel, radar operators and maintenance personnel, radio/TV antenna maintenance and repair workers, dielectric welders and plastic sealers, and physiotherapists applying diathermy treatments. Exposures within the occupational limits of ICNIRP [1] belong to low-level exposures with a maximum psSAR10g of 10 W/kg and wbSAR of 0.4 W/kg. Numerical simulations predict that the local temperature increase remains below 3.2 °C anywhere in the body [15••, 16–18], below 1.2 °C in the brain [18–21], and below 0.12 °C in body core temperature [12, 17].

The corresponding values for the general public are five times lower. The risks of long-term or chronic exposures below the ICNIRP guidelines were recently evaluated by IARC, resulting in the controversial classification of the exposure as "Group 2B possibly carcinogenic to humans" [22]. Acute effects on human EEG (waking and sleep), cerebral blood flow, and cognitive performance [23] have been reported in different laboratories; however, the underlying mechanisms have not yet been identified.

High-Level RF Exposure and Thermal Dose

MRI exposure can be an order of magnitude higher than occupational exposure and nearly 50 times higher than the guidelines for the general public, namely wbSAR >3 W/kg and psSAR10g >80 W/kg [13•, 24]. This may induce considerable systemic thermal stress and initiate both whole-body thermoregulation [25, 26] and local thermoregulation processes around thermal hotspots [12, 13•]. There are supposedly three fundamental physiological responses to excessive heat in the human body: (a) whole-body systemic thermoregulation which keeps the body core temperature stable via a generally increased skin and extremity perfusion, sweating, and decrease in metabolic rate, (b) local cutaneous perfusion increase in response to local or superficial heating, and (c) local thermoregulatory responses in inner tissues and organs, which has the highest model uncertainty due to very limited knowledge [12]. There are many complex interactions between these three responses, e.g., related to the overall limited amount of blood, which will not be discussed further.

The human body has a remarkable ability to maintain a stable body core temperature. Data from hyperthermia applications show that even exposures up to a wbSAR of 10 W/kg for 30–60 min generally do not cause increases in body core temperatures above 38 °C, and rarely above 39 °C [27] for patients without fever. Skin tissues have the potential to up-regulate blood-flow by a factor of up to 32, which has often been underestimated [12]. The situation with internal organs and tissues is least investigated so far. Again data from hyperthermia applications indicate a high perfusion increase in healthy internal tissues. Laakso et al. [12] estimate an increase of up to a factor of 15. There are potentially high inter-individual differences, and some patient groups may have a pathologically impaired thermoregulatory response. Murbach et al. [28] proposed a model with a 70 % reduced thermoregulatory perfusion-response in certain patient groups.

Considering these thermoregulatory response-models, local temperatures still may exceed 42 °C in muscle or skin tissues [13•, 27]. Additionally, the local RF absorption can reach significantly higher magnitudes when the body comes into close proximity of stray fields around the capacitors of the birdcage; when the body forms anatomical RF current loops; or at the electrodes of metal components within the implants, as discussed below.

Systemic thermal stress in the patient can be easily detected by monitoring heart rate, core temperature elevation, or the patient's subjective well-being. Special precautions must be taken for non-responsive patients (e.g., anesthetized, sedated, or infant patients). For local exposures, however, local temperatures may not be adequately perceived due to limited heat sensation (e.g., in muscle tissue) [29]. Actual tissue stress and damage result from a combination of induced temperature increases and exposure-duration. The thermal dose model of cumulative equivalent minutes at 43 °C (CEM43) was first proposed in 1984 by Sapareto et al. [30] and allows any transient temperature profile to be converted into equivalent minutes of heating at 43 °C. In combination with tissue specific damage thresholds [31, 32, 33••], CEM43 may constitute an adequate model to predict tissue damage (major or minor) over a wide range of exposure temperatures. Evaluations of CEM43 data for MRI applications [33••] resulted in a proposed damage threshold of CEM43 = 16 min for skin, muscle, fat, and bone. These tissues can sustain 16 min at 43 °C, which can be translated, e.g., to 8 min at 44 °C, 32 min at 42.5 °C, 64 min at 42 °C, or 256 min at 41° C. Temperatures below 39 °C were considered safe for any duration. Considering the remarkable HoSU in MRI scanning, it is likely that these thermal doses were not reached. At the same time, full exploitation of the guideline limits (4 W/kg for prolonged scans, e.g., 60 min) may lead to thermal doses above CEM43 = 16 min in some patients and imaging positions [13•, 14], and may even exceed CEM43 = 500 min in animal experiments [34••]. However, due to frequent scan interruptions and the manufacturer's safety margin, the vast majority of clinical MRI scans will not reach the maximal allowed exposure limits [35–37]. In current clinical practice, scanner-indicated wbSAR levels above 3.5 W/kg are only reached for 5 min on average, with 50 % of all scans lasting between 3 and 9 min [4], which extrapolates to 0.1 % of scans with high wbSAR for more than 23 min.

The scanner-indicated wbSAR levels do not include the manufacturer's safety margin. Thus, the HoSU over the last 30 years may not be attributable to the maximum allowance of the IEC product standard, but rather to the actual applied exposures, which can be, and often are, considerably lower.

Numerical Simulations for RF Safety Assessment in MRI

As internal field quantities cannot be directly measured in humans, numerical simulations have become the method of choice to conduct RF safety assessments. Validated in silico methods are used to estimate the induced RF field distributions in vivo by creating relevant simulation models. The first step is to reproduce a realistic RF incident field (or B1 field) of the MRI RF coil model. B1 should (a) be circularly polarized around the static magnetic field axis to effectively cause the nutation of nuclear spins, (b) have high intensity to maximize the transmit efficiency, and (c) be highly uniform for homogeneous contrast. A streamline view of B1 is depicted in Fig. 1. While the body coils at 1.5 T are typically driven in circular polarization, exposures at 3 T and above may have higher degrees of freedom (RF shimming and pTx, typically 2–32 ports), considerably complicating the estimation of local SAR [5•, 8, 38–41]. The next step is to assign tissue dielectric and thermal properties based on literature values [11, 42] and compute the induced fields within the human anatomical models. An example of the SAR distribution is shown in Fig. 2. The final step is to translate the induced RF energy to a temperature increase via thermal simulations. The thermal response at high SAR exposure locations depends mainly on the perfusion and local thermoregulation [12], the parameters of which have not been determined with well-characterized uncertainty bounds. Additional studies on the variations of thermally induced perfusion changes must be conducted to validate the currently applied simplified models [43]. An example of RF-induced elevated skin temperatures is depicted in Fig. 3. Thermal tissue damage can be estimated via thermal dose models, as described earlier.

For all of the above steps, a detailed uncertainty and sensitivity analysis is necessary for determining the dominant factors affecting SAR, temperature, and thermal dose [12, 13•, 44].

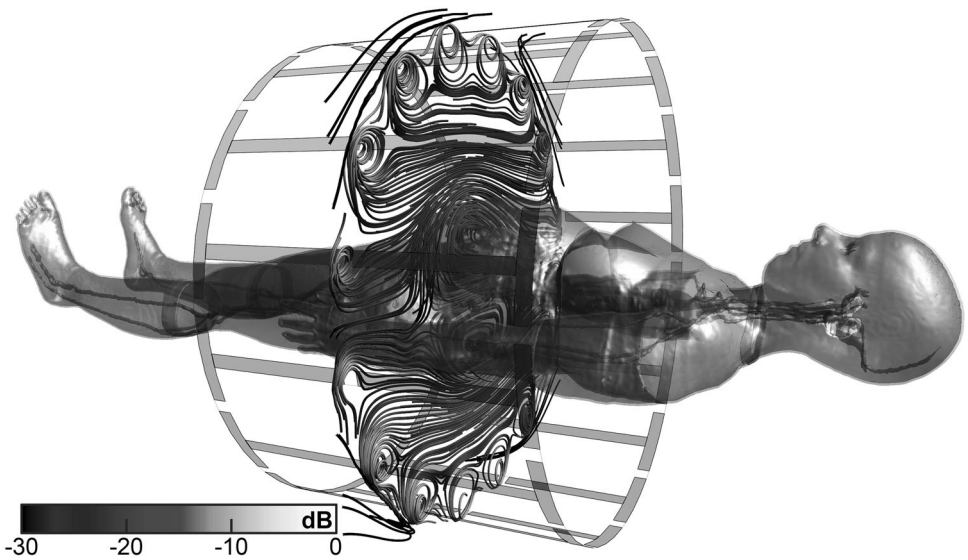

Fig. 1 Streamline view of the B1 RF field of a birdcage body coil at 3 T with a pregnant anatomical model in the fetal imaging position. B1 should be highly uniform within the region of interest (*parallel streamlines*)

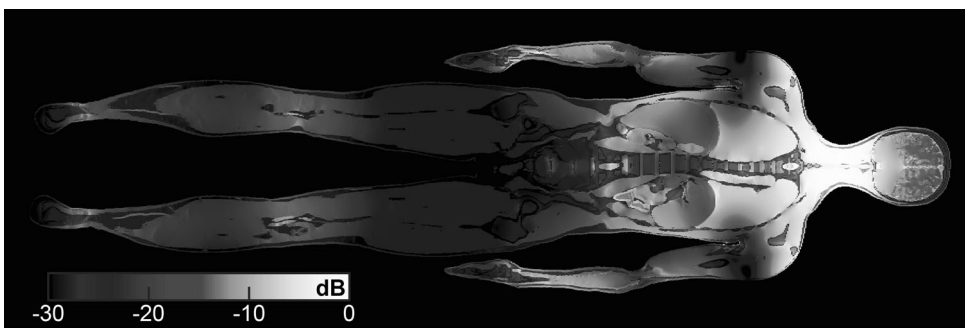

Fig. 2 SAR distribution in the upper sternum of the anatomical model Louis. High SAR is reached around the neck-shoulder region

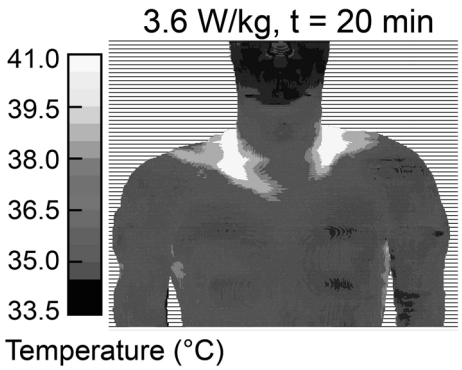

Fig. 3 Numerically estimated surface temperature in the upper sternum of the anatomical model Duke after heating with wbSAR = 3.6 W/kg for 20 min. High temperatures are reached around the RF hotspots in the neck-shoulder region

Experimental Thermal Validations

Experimental validation of in vivo temperatures is challenging. MR thermometry, which utilizes the proton resonance frequency shift (PRFS) [45], can be applied to assess tissue temperature changes over the baseline directly via the scanner. Although the quality, speed, and accuracy of MR thermometry are continually increasing [46], issues such as limited functionality in some tissues (e.g., fat), high susceptibility to motion artifacts, and perfusion changes still exist. A recent temperature increase experiment in the human forearm [47, 48], comparing MR thermometry measurements with simulated thermal responses, represents a promising step towards the validation of thermal simulations in MRI. Although the model prediction must be further refined, good agreement has been achieved between simulations and measurements with high SAR exposures (psSAR10g presumably above 200 W/kg for 2 min).

Investigations on the thermal steady state and thermoregulated local blood perfusion can provide valuable data for future studies. Measurements with temperature probes attached to the skin at estimated hotspots were performed at two different realistic exposure levels in [13•]. The applied thermoregulation model reproduced the steady-state behavior of the hotspots with good accuracy. However, skin measurements alone do not validate internal muscle temperatures, where MR thermometry is the only non-invasive option.

Recent animal studies have investigated MRI exposure with temperature increases [49], including thermal dose and actual histopathological tissue damage [34••]. In those experiments, exposures in porcine muscle within the IEC limits (wbSAR = 3.7 W/kg) led to thermal doses up to CEM43 >500 min, resulting in tissue damage. Whether these results are transferable to humans remains an open question, as porcine thermoregulation may be very different, especially when under anesthesia. However, experiments in swine are indispensable: among available experimental animals, the pig is the most similar to human. Due to differences in heart volume and capillary density, the pig model seems to be more conservative in terms of local temperatures [34••].

Concepts for Safety Supervision

Currently, RF safety supervision in MRI systems is heavily based on SAR considerations. IEC 60601-2-33 only specifies average SAR limits for volume coils, which may not be sufficiently conservative to control local temperature increases. Alternative methodologies are being evaluated. Promising concepts include:

- more conservative SAR limits that would prevent the prolonged high SAR exposures currently allowed by full exploitation of the current standard. Results from thermal dose-based evaluations indicate that these more conservative SAR limits may be sufficient to ensure compliance with the current temperature limits [13•]; although this approach is easy to implement, high safety margins may be applied to guarantee conservativeness;
- direct MR thermometry measurement, as currently applied in thermal therapy [50]; direct supervision of the hotspot temperatures would constitute a very safe method; however, additional thermometry scans are necessary and, for certain scenarios, the hotspot may occur outside of the field of view;
- patient-specific exposure estimations: (a) using gross anatomical properties [51], (b) by mapping the patient to a similar anatomical model, or (c) actual patient anatomy with ad hoc segmentation [52]. This is an elegant method to gain broad insight into the induced RF fields, and may result in lower safety margins. However, considerable computational time may be required.
- B1+ scanner measurements and subsequent reconstruction of the B1 field [53]; the additional B1+ scans may contain insufficient information to fully reconstruct the induced field; and
- thermo-acoustic SAR estimation using very sharp RF pulses [54]; some feasibility studies are currently being conducted at this early stage of development.

Safety Considerations Regarding RF-Induced Heating for Patients with Implants

Patients with metallic or conductive implants present additional safety challenges. As relatively large levels of RF fields are induced in the human body during MRI,

metallic passive and active implants can collect the RF power like antennas, resulting in induced currents along the conductive structure and creating local hotspots at the implant–tissue interface. The amount of implant-induced tissue heating can be significant, i.e., $\gg$10 °C [55] for elongated conductive implants with isolated leads and open electrodes, such as cardiac pacemakers and defibrillator leads [56, 57] and neurostimulator leads [58, 59]. The described risk due to RF-induced heating also applies to passive implants with conductive elongated components such as metallic stents and abandoned leads, whereas non-conductive and short conductive implants present a lower risk; however, dimension and conductivity thresholds must still be assessed.

Implants with mostly insulated bodies and open metallic electrode contacts, such as active cardiac- and neuro-stimulation devices, can deposit the collected RF power very locally and lead to significant heating of tissue at the electrode-tissue interface [60]. The magnitude of the locally deposited power or RF heating depends on a multitude of conditions:

(i) the specific design features of the MRI system (e.g., RF coil design and manufacturer's power calculation algorithms) [61];
(ii) the implant (specific designs, i.e., material, equivalent RF impedance; effective electrical length; and resistive/component losses) [57, 62, 63];
(iii) the implant clinical routing (e.g., tissue distribution along the trajectory) [64••];
(iv) the patient (e.g., patient anatomy and posture); and
(v) the patient position within the RF coil [65].

For active implants, certain conditions can enhance or reduce the risks. Hence, the risks cannot be assessed without a detailed analysis considering a sufficient combination of the different conditions. In this context, studies that have reported no adverse effects in patients with specific implants (e.g., cardiac rhythm devices [66, 67]) have limited value as such studies may not have necessarily included the major risk factors that only occur for a very specific combination of the above conditions. The latest standard ISO/TS 10974 [68] describes the procedures to determine most of the above conditions and Cabot et al. [55] demonstrated the utility of the proposed procedures; however, certain factors including tissue distribution along the trajectory, boundary effects, coupling between different leads, coupling between different lead sections from lead-coiling, ohmic losses, and uncertainty assessments have not been fully addressed yet. At present, the ISO/TS 10974 does not address the risk of body-mounted and partially implanted devices (e.g., ECG electrodes and interventional catheters). The associated health risks are evaluated in terms of thermal [69, 70] and other physiological thresholds (e.g., pacing capture threshold in cardiac stimulation devices [65]). Nevertheless, while substantial tissue heating in the vicinity of a cardiac pacemaker may be tolerated and may not cause consistently detectable histological alterations [56], a relatively small temperature increase in brain tissue induced by a deep brain stimulator may be detrimental, thus emphasizing the importance of tissue specific damage thresholds.

For passive implants, the ASTM F2182 [71] provides guidelines for testing the tissue heating during MRI RF exposure and RF-related heating of a significant number of passive implants (e.g., vascular stents [72–74], orthopedic implants [75–77], dental implants [78], and small surgical clips [79]). In this test method, the implant is exposed to a uniform electric field over the extent of the implant and the in vitro temperature increase reported. This testing criterion is only suitable for the evaluation of electrically small implants, i.e., implant dimensions much smaller than the effective wavelength in media, where no significant phase variation of the incident field along the implant is expected during MRI exposure. Comprehensive test requirements, including incident or test field conditions, evaluations as a function of the electrical length of the implants, and translation from in vitro assessments to in vivo estimates that are independent of the test institutions, have yet to be established.

In general, for non-conductive and non-metallic implants there is very limited risk due to induced RF [80, 81]. A systematic evaluation of potential risks due to current displacements is still lacking.

The amount of implant-induced RF heating depends on the RF field strengths that expose the implant and the implant's propensity to capture that RF energy. Several studies have reported techniques for heating mitigation through a careful design of RF exposure during MRI [64••, 82]. Alternatively, several lead modification techniques may reduce the ability of implant leads to collect the RF energy [83–85].

Conclusions

Excessive thermal dose is the main RF safety concern in MRI. The HoSU for MRI includes minimal data on scans that fully exploit the IEC 60601-2-33 exposure limits. The basic (temperature) and derived (SAR) safety limits are currently inconsistent in IEC 60601-2-33, as temperatures >40 °C are likely to be induced if the current SAR limitation is fully exploited [13•, 14, 34••, 49]. Further investigations on the safety of high-level RF scans and the safety of MRI in patients with impaired thermoregulation are needed. Additionally, emerging MRI technologies (such as parallel transmissions systems) and the growing number of patients with medical implants that require MRI scans are making MRI safety assessments more challenging.

Numerical simulations using high-resolution anatomical and functionalized human models and powerful electromagnetic and thermal solvers together with tissue models are newly available tools that allow the open safety questions to be addressed and may assist in the development of new safety concepts. These tools must be further improved to include a more detailed characterization of anatomical and functional variations based on improved tissue models and parameters. Knowledge about the potential risks of patients with implantable medical devices from RF heating has grown substantially in recent years and novel methodologies to evaluate the risks have been developed; however, patient safety can only be fully ensured and unacceptable risks for specific patient groups can only be excluded by establishing complete evaluation techniques. Sound experimental verification and validation procedures and thorough uncertainty assessments are vital to ensure the reliability and accuracy of the safety assessments.

Disclaimer

Dr. Kainz's role in this article was completed outside of his duties at the US Food and Drug Administration. The views expressed do not represent the views of the agency or the US government. In addition, the content of this report is solely the responsibility of the authors and does not necessarily represent the official views of the National Institutes of Health.

Compliance with Ethics Guidelines

Conflict of Interest Prof. Niels Kuster reports grants from CTI - Commission for Technology and Innovation, Switzerland, grants from Schmid & Partner Engineering AG, Switzerland, grants from ZMT Zurich MedTech AG, Switzerland, grants from Siemens Health Care GmbH, Germany, grants from GE Medical Systems, USA, during the conduct of the study; other from Boston Scientific Corp., USA, other from Micro Systems Engineering Inc., USA, other from Med-El, Austria, other from Sorin CRM S.A.S., France, other from Nevro Corp., USA, other from St. Jude Medical Inc., USA.

Human and Animal Rights and Informed Consent This article does not contain any studies with human or animal subjects performed by any of the authors.

References

Papers of particular interest, published recently, have been highlighted as:
- • Of importance
- •• Of major importance

1. ICNIRP. Guidelines for limiting exposure to time-varying electric, magnetic, and electromagnetic fields (up to 300 GHz). Health Phys. 1998;74:494–522.
2. IEC. Medical electrical equipment—particular requirements for the basic safety and essential performance of magnetic resonance equipment for medical diagnosis, Edition 3.2. IEC 60601-2-33:2010 + AMD1:2013 + AMD2:2015 CSV 2015.
3. Luechinger R. MRI safety. In: Syed MA, Mohiaddin RH, editors. Magnetic resonance imaging of congenital heart disease. New York: Springer; 2012. p. 39–46.
4. Langman DA, Srinivasan S, Ennis D. What is the SAR for routine clinical MRI exams at 1.5 T? Proc Intl Soc Magn Reson Med. 2015;23:0302.
5. • Guérin B, Gebhardt M, Serano P, Adalsteinsson E, Hamm M, Pfeuffer J, Nistler J, Wald LL. Comparison of simulated parallel transmit body arrays at 3 T using excitation uniformity, global SAR, local SAR, and power efficiency metrics. Magn Reson Med. 2014;1150:1137–50. *Application study, evaluating SAR exposures as a function of different pTx body array coils and their excitations.*
6. Brunner DO, Pruessmann KP. Optimal design of multiple-channel RF pulses under strict power and SAR constraints. Magn Reson Med. 2010;63:1280–91.
7. Malik SJ, Beqiri A, Padormo F, Hajnal JV. Direct signal control of the steady-state response of 3D-FSE sequences. Magn Reson Med. 2014;73:951–63.
8. Van Osch MJP, Webb AG. Safety of ultra-high field MRI: what are the specific risks? Curr Radiol Rep. 2014;2:61.
9. Christ A, Kainz W, Hahn EG, et al. The virtual family—development of surface-based anatomical models of two adults and two children for dosimetric simulations. Phys Med Biol. 2010;55:N23–38.
10. Gosselin M-C, Neufeld E, Moser H, et al. Development of a new generation of high-resolution anatomical models for medical device evaluation: the virtual population 3.0. Phys Med Biol. 2014;59:5287–303.
11. Hasgall PA, Di Gennaro F, Baumgartner C, Neufeld E, Gosselin MC, Payne D, Klingenböck A, Kuster N. IT'IS database for thermal and electromagnetic parameters of biological tissues. Version 2.5. www.itis.ethz.ch/database (2014). Accessed 1 Aug 2014
12. Laakso I, Hirata A. Dominant factors affecting temperature rise in simulations of human thermoregulation during RF exposure. Phys Med Biol. 2011;56:7449–71.
13. • Murbach M, Neufeld E, Capstick M, Kainz W, Brunner DO, Samaras T, Pruessmann KP, Kuster N. Thermal tissue damage model analyzed for different hole-body SAR and scan durations for standard MR body coils. Magn Reson Med. 2014;71:421–31. *Concept of thermal dose (CEM43) evaluation in MRI exposures, using various anatomical human models in different imaging positions.*
14. Nadobny J, Szimtenings M, Diehl D, Stetter E, Brinker G, Wust P. Evaluation of MR-induced hot spots for different temporal SAR modes using a time-dependent temperature gradient treatment. IEEE Trans Biomed Eng. 2007;54:1837–50.
15. •• Neufeld E, Fuetterer M, Murbach M, Kuster N. Rapid method for thermal dose-based safety supervision during MR scans. Bioelectromagnetics. 2015;36:398–407. *Methodology for the rapid assessment of thermal dose in MR-scanning, based on the actual SAR sequence of the scanner.*
16. Fujimoto M, Hirata A, Wang J, Fujiwara O, Shiozawa T. FDTD-derived correlation of maximum temperature increase and peak SAR in child and adult head models due to dipole antenna. IEEE Trans Electromagn Compat. 2006;48:240–7.
17. Hirata A, Laakso I, Oizumi T, Hanatani R, Chan KH, Wiart J. The relationship between specific absorption rate and temperature elevation in anatomically based human body models for plane wave exposure from 30 MHz to 6 GHz. Phys Med Biol. 2013;58:903–21.
18. Hirata A, Shiozawa T. Correlation of maximum temperature increase and peak SAR in the human head due to handset antennas. IEEE Trans Microw Theory Tech. 2003;51:1834–41.

19. Collins CM, Liu W, Wang J, Gruetter R, Vaughan JT, Ugurbil K, Smith MB. Temperature and SAR Calculations for a human head within volume and surface coils at 64 and 300 MHz. J Mag Res Imag. 2004;19:650–6.
20. Wang Z, Lin JC, Mao W, Liu W, Smith MB, Collins CM. SAR and temperature: simulations and comparison to regulatory limits for MRI. J Mag Res Imag. 2007;26:437–41.
21. Samaras T, Kalampaliki E, Sahalos JN. Influence of thermo-physiological parameters on the calculations of temperature rise in the head of mobile phone users. IEEE Trans Electromagn Compat. 2007;49:936–9.
22. IARC. IARC Monographs Vol. 102. Non-ionizing radiation. Part 2: Radiofrequency electromagnetic fields. 2013;102:460.
23. Loughran SP, McKenzie RJ, Jackson ML, Howard ME, Croft RJ. Individual differences in the effects of mobile phone exposure on human sleep: rethinking the problem. Bioelectromagnetics. 2012;33:86–93.
24. Murbach M, Cabot E, Neufeld E, Gosselin M-C, Christ A, Kuster N. Local SAR enhancements in anatomically correct children and adult models as a function of position within 1.5 T MR body coil. Prog Biophys Mol Biol. 2011;107:428–33.
25. Abart J, Brinker G, Irlbacher W, Grebmeier J. Temperature and heart rate changes in MRI at SAR levels of up to 3 W/kg. Proc Intl Soc Magn Reson Med. 1989;998.
26. Adair ER, Berglund LG. Predicted thermophysiological responses of humans to MRI fields. Ann N Y Acad Sci. 1992;649: 188–200.
27. Wust P, Nadobny J, Szimtenings M, Stetter E, Gellermann J. Implications of clinical RF hyperthermia on protection limits in the RF range. Health Phys. 2007;92:565–73.
28. Murbach M, Neufeld E, Cabot E, Zastrow E, Juan C, Kainz W, Kuster N. Virtual Population-based assessment of the impact of 3 Tesla radiofrequency shimming and thermoregulation on safety and B1+ uniformity. Magn Reson Med. 2015. doi:10.1002/mrm.25986.
29. Graven-Nielsen T, Arendt-Nielsen L, Mense S. Thermosensitivity of muscle: high-intensity thermal stimulation of muscle tissue induces muscle pain in humans. J Physiol. 2002;540:647–56.
30. Sapareto SA, Dewey WC. Thermal dose determination in cancer therapy. Int J Radiat Oncol Biol Phys. 1984;10:787–800.
31. Dewhirst MW, Viglianti BL, Lora-Michiels M, Hanson M, Hoopes PJ. Basic principles of thermal dosimetry and thermal thresholds for tissue damage from hyperthermia. Int J Hyperth. 2003;19:267–94.
32. Yarmolenko PS, Moon EJ, Landon C, Manzoor A, Hochman DW, Viglianti BL, Dewhirst MW. Thresholds for thermal damage to normal tissues: an update. Int J Hyperth. 2011;27:320–43.
33. •• Van Rhoon GC, Samaras T, Yarmolenko PS, Dewhirst MW, Neufeld E, Kuster N. CEM43 °C thermal dose thresholds: a potential guide for magnetic resonance radiofrequency exposure levels? Eur Radiol. 2013;23:2215–27. *Proposed thermal damage thresholds for MR exposures, which considers the risk/benefit considerations. Data is originating from multiple sources including experience from hyperthermia.*
34. •• Nadobny J, Klopfleisch R, Brinker G, Stoltenburg-Didinger G. Experimental investigation and histopathological identification of acute thermal damage in skeletal porcine muscle in relation to whole-body SAR, maximum temperature, and CEM43 C due to RF irradiation in an MR body coil of birdcage type at 123 MHz. Int J Hyperthermia. 2015;31:409–20. *Experimental heating study in swine, demonstrating local tissue damage from exposure-levels currently allowed by the safety standard.*
35. Hand JW, Li Y, Hajnal JV. Numerical study of RF exposure and the resulting temperature rise in the foetus during a magnetic resonance procedure. Phys Med Biol. 2010;55:913–30.
36. Hand JW, Li Y, Thomas EL, Rutherford MA. Prediction of specific absorption rate in mother and fetus associated with MRI examinations during pregnancy. Magn Reson Med. 2006;55: 883–93.
37. Hand JW, Lagendijk JJW, Hajnal JV, Lau RW, Young IR. SAR and temperature changes in the leg due to an RF decoupling coil at frequencies between 64 and 213 MHz. J Magn Reson Imaging. 2000;12:68–74.
38. Beqiri A, Hand JW, Hajnal JV, Malik SJ. Comparison between simulated decoupling regimes for specific absorption rate prediction in parallel transmit MRI. Magn Reson Med. 2015;74: 1423–34.
39. Carluccio G, Collins CM, Erricolo D. A fast, analytically based method to optimize local transmit efficiency for a transmit array. Magn Reson Med. 2014;71:432–9.
40. Eryaman Y, Guerin B, Keil B, et al. SAR reduction in 7 T C-spine imaging using a "dark modes" transmit array strategy. Magn Reson Med. 2015;73:1533–9.
41. Guérin B, Setsompop K, Ye H, Poser BA, Stenger AV. Design of parallel transmission pulses for simultaneous multislice with explicit control for peak power and local specific absorption rat. Magn Reson Med. 2014;73:1946–53.
42. Gabriel S, Lau R, Gabriel C. The dielectric properties of biological tissues: II. measurements in the frequency range 10 Hz to 20 GHz. Phys Med Biol. 1996;41:2251–69.
43. Mathewson KW, Haykowsky MJ, Thompson RB. Feasibility and reproducibility of measurement of whole muscle blood flow, oxygen extraction, and VO2 with dynamic exercise using MRI. Magn Reson Med. 2015. doi:10.1002/mrm.25564.
44. Shao Y, Zeng P, Wang S. Statistical simulation of SAR variability with geometric and tissue property changes by using the unscented transform. Magn Reson Med. 2014;2362:2357–62.
45. Lüdemann L, Wlodarczyk W, Nadobny J, Weihrauch M, Gellermann J, Wust P. Non-invasive magnetic resonance thermography during regional hyperthermia. Int J Hyperth. 2010;26:273–82.
46. Gaur P, Grissom WA. Accelerated MRI thermometry by direct estimation of temperature from undersampled k-space data. Magn Reson Med. 2014;1925:1914–25.
47. Oh S, Ryu YC, Carluccio G, Sica CT, Collins CM. Measurement of SAR-induced temperature increase in a phantom and in vivo with comparison to numerical simulation. Magn Reson Med. 2013;1931:1923–31.
48. Cao Z, Oh S, Otazo R, Sica CT, Griswold MA, Collins CM. Complex difference constrained compressed sensing reconstruction for accelerated PRF thermometry with application to MRI-induced RF heating. Magn Reson Med. 2015;73:1420–31.
49. Shrivastava D, Utecht L, Tian J, Hughes J, Vaughan JT. In vivo radiofrequency heating in swine in a 3 T (123.2-MHz) birdcage whole body coil. Magn Reson Med. 2013;1150:1141–50.
50. Rieke V, Pauly KB. MR thermometry. J Magn Reson Imaging. 2008;27:376–90.
51. Murbach M, Neufeld E, Kainz W, Pruessmann KP, Kuster N. Whole-body and local RF absorption in human models as a function of anatomy and position within 1.5 T MR body coil. Magn Reson Med. 2014;71:839–45.
52. Homann H, Börnert P, Eggers H, Nehrke K, Dössel O, Graesslin I. Toward individualized SAR models and in vivo validation. Magn Reson Med. 2011;66:1767–76.
53. Voigt T, Homann H, Katscher U, Doessel O. Patient-individual local SAR determination: in vivo measurements and numerical validation. Magn Reson Med. 2012;68:1117–26.
54. Winkler SA, Picot P, Thronton M, Rutt BK. Direct SAR mapping by thermoacoustic imaging: experimental proof-of-concept. Proc Intl Soc Magn Reson Med. 2015;23:3234.
55. Cabot E, Lloyd T, Christ A, Kainz W, Douglas M, Stenzel G, Wedan S, Kuster N. Evaluation of the RF heating of a generic deep brain stimulator exposed in 1.5 T magnetic resonance scanners. Bioelectromagnetics. 2013;34:104–13.

56. Luechinger R, Zeijlemaker VA, Pedersen EM, Mortensen P, Falk E, Duru F, Candinas R, Boesiger P. In vivo heating of pacemaker leads during magnetic resonance imaging. Eur Heart J. 2005;26:376–83.
57. Mattei E, Calcagnini G, Censi F, Triventi M, Bartolini P. Radiofrequency dosimetry in subjects implanted with metallic straight wires: a numerical study. Conf Proc Int Conf IEEE Eng Med Biol Soc. 2008;2008:4387–90.
58. Henderson JM, Tkach J, Phillips M, Baker K, Shellock FG, Rezai AR. Permanent neurological deficit related to magnetic resonance imaging in a patient with implanted deep brain stimulation electrodes for Parkinson's disease: case report. Neurosurgery. 2005;57:E1063, discussion E1063.
59. Spiegel J, Fuss G, Backens M, Reith W, Magnus T, Becker G, Moringlane J-R, Dillmann U. Transient dystonia following magnetic resonance imaging in a patient with deep brain stimulation electrodes for the treatment of Parkinson disease. Case report. J Neurosurg. 2003;99:772–4.
60. Acikel V, Atalar E. Modeling of radio-frequency induced currents on lead wires during MR imaging using a modified transmission line method. Med Phys. 2011;38:6623.
61. Baker KB, Tkach JA, Phillips MD, Rezai AR. Variability in RF-induced heating of a deep brain stimulation implant across MR systems. J Magn Reson Imaging. 2006;24:1236–42.
62. Nordbeck P, Weiss I, Ehses P, et al. Measuring RF-induced currents inside implants: impact of device configuration on MRI safety of cardiac pacemaker leads. Magn Reson Med. 2009;61:570–8.
63. Bottomley PA, Kumar A, Edelstein WA, Allen JM, Karmarkar PV. Designing passive MRI-safe implantable conducting leads with electrodes. Med Phys. 2010;37:3828–43.
64. •• Corcoles J, Zastrow E, Kuster N. Convex optimization of MRI exposure for mitigation of RF-heating from active medical implants. Phys Med Biol. 2015;60:7293–308. *Introduction of a technique for heating mitigation through a careful design of RF exposure during MRI, considering the clinical routing of the implant*.
65. Wilkoff BL, Albert T, Lazebnik M, et al. Safe magnetic resonance imaging scanning of patients with cardiac rhythm devices: a role for computer modeling. Heart Rhythm. 2013;10:1815–21.
66. Gold MR, Sommer T, Schwitter J, et al. Full-body MRI scanning in patients with an ICD: primary results of the randomized Evera MRI study. J Am Coll Cardiol. 2015;65:2589–90.
67. Gimbel JR, Bello D, Schmitt M, et al. Randomized trial of pacemaker and lead system for safe scanning at 1.5 Tesla. Heart Rhythm. 2013. doi:10.1016/j.hrthm.2013.01.022.
68. ISO/TS. 10974:2012, Requirements for the safety of magnetic resonance imaging for patients with an active implantable medical device. ISO/TS 10974 2012.
69. Gupte AA, Shrivastava D, Spaniol MA, Abosch A. MRI-related heating near deep brain stimulation electrodes: more data are needed. Stereotact Funct Neurosurg. 2011;89(3):131–40.
70. Gorny KR, Presti MF, Goerss SJ, et al. Measurements of RF heating during 3.0-T MRI of a pig implanted with deep brain stimulator. Magn Reson Imaging. 2013;31:783–88.
71. ASTM. F2182-11a. Standard test method for measurement of radio frequency induced heating near passive implants during magnetic resonance imaging. 2011:1–8.
72. Shellock FG, Shellock VJ. Metallic stents: evaluation of MR imaging safety. Am J Roentgenol. 1999;173(3):543–7.
73. Camps-Raga B, Goertz W, Schaefers G, Mezape Y, Shalev A. A comparative study of numerical and experimental evaluation of RF-induced heating for an endovascular stent-graft at 1.5 T and 3 T. Biomed Eng. 2012;57:4348.
74. Titterington B, Puschmann C, Shellock FG. A new vascular coupling device: assessment of MRI issues at 3-tesla. Magn Reson Imaging. 2014;32(5):585–9.
75. Kumar R, Lerski RA, Gandy S, Clift BA, Abboud RJ. Safety of orthopedic implants in magnetic resonance imaging: an experimental verification. J Orthop Res. 2006;24(9):1799–802.
76. Zou Y, Chu B, Wang C, Hu Z. Evaluation of MR issues for the latest standard brands of orthopedic metal implants: plates and screws. Eur J Radiol. 2015;84(3):450–7.
77. Liu Y, Chen J, Shellock FG, Kainz W. Computational and experimental studies of an orthopedic implant: MRI-related heating at 1.5-T/64-MHz and 3-T/128-MHz. J Mag Res Imag. 2013;37:491–7.
78. Hasegawa M, Miyata K, Abe Y, Ishigami T. Radiofrequency heating of metallic dental devices during 3.0 T MRI. Dentomaxillofacial Radiol. 2013;42(5):1–6.
79. Gill A, Shellock FG. Assessment of MRI issues at 3-Tesla for metallic surgical implants: findings applied to 61 additional skin closure staples and vessel ligation clips. J Cardiovasc Magn Reson. 2012;14:3.
80. ASTM. F2503-11. Standard practice for marking medical devices and other items for safety in the magnetic resonance environment. 2013:1–7.
81. Shellock FG, Woods TO, Crues JV. MR labeling information for implants and devices: explanation of terminology. Radiology. 2009;253(1):26–30.
82. Eryaman Y, Guerin B, Akgun C, et al. Parallel transmit pulse design for patients with deep brain stimulation implants. Magn Reson Med. 2014;73:1896–903.
83. Ladd ME, Quick HH. Reduction of resonant RF heating in intravascular catheters using coaxial chokes. Magn Reson Med. 2000;43:615–9.
84. Gray RW, Bibens WT, Shellock FG. Simple design changes to wires to substantially reduce MRI-induced heating at 1.5 T: implications for implanted leads. Magn Reson Imaging. 2005;23:887–91.
85. Weiss S, Vernickel P, Schaeffter T, Schulz V, Gleich B. Transmission line for improved RF safety of interventional devices. Magn Reson Med. 2005;54:182–9.